


## Article

# Design and Implementation of a Land-Air Omnidirectional Mobile Robot

Changlong Ye <sup>1</sup> , Hongyu Wang <sup>1</sup>, Suyang Yu <sup>1,\*</sup>, Xinyu Ma <sup>1</sup> and Ruizhe Zhou <sup>2</sup>

<sup>1</sup> School of Mechatronics Engineering, Shenyang Aerospace University, Shenyang 110135, China; changlye@163.com (C.Y.); wahoyuu@126.com (H.W.); maxinyu18204267066@163.com (X.M.)

<sup>2</sup> Electrical and Computer Engineering Department, Rose-Hulman Institute of Technology, Terre Haute, IN 47803, USA; richard\_zrz@126.com

\* Correspondence: yu\_suyang@163.com or yu\_suyang@sau.edu.cn

**Abstract:** This paper proposes a new type of omnidirectional mobile robot for land and air, which has three motion modes, combines the motion characteristics of land motion and air flight, has the ability to climb walls, and can be actively deformed to adapt to the working conditions according to the current working environment. The robot incorporates an innovative “rotor blade–single row omnidirectional wheel” composite structure, which is mainly characterized by a single row of continuous switching wheels covering the outside of each rotor blade, and does not need to provide additional power when moving on the ground and walls, relying on the driving force generated by the rotor blades to drive the continuous switching wheels driven by the rotor blades. This structure can effectively combine the land movement mode, wall crawling mode, and air flight mode, which reduces the energy consumption of the robot without increasing the weight, and we design a deformation device that can realize the transformation of the three modes into each other. This paper mainly focuses on the design of the robot structure and the analysis of the movement method, and the land omnidirectional movement experiments, wall crawling experiments, and air flight experiments were, respectively, carried out, and the results show that the proposed land and air omnidirectional mobile robot has the ability to adapt to the movement of each scene, and improves the upper limit of the robot’s operation.

**Keywords:** land–air; omnidirectional mobility; multi-modal robots; wing–wheel composite; motion pattern analysis



**Citation:** Ye, C.; Wang, H.; Yu, S.; Ma, X.; Zhou, R. Design and

Implementation of a Land-Air Omnidirectional Mobile Robot.

*Aerospace* **2024**, *11*, 576. <https://doi.org/10.3390/aerospace11070576>

Academic Editor: Hoang-Vu Phan

Received: 9 May 2024

Revised: 9 July 2024

Accepted: 11 July 2024

Published: 14 July 2024



**Copyright:** © 2024 by the authors. Licensee MDPI, Basel, Switzerland. This article is an open access article distributed under the terms and conditions of the Creative Commons Attribution (CC BY) license (<https://creativecommons.org/licenses/by/4.0/>).

## 1. Introduction

Mobile robots are widely used to explore or perform search and rescue missions in a variety of unstructured environments [1–4], replacing humans to improve the completeness of operations in such environments. For example, in buildings or underground tunnels that pose safety hazards after disasters, there is a possibility of triggering secondary accidents during manual search and rescue. Human movement is limited in extraterrestrial exploration. There is a high risk of manual exploration in environments that are flammable, explosive, toxic, or hazardous.

In recent years, frequent natural disasters and conflicts, such as the Russia–Ukraine war, the Israel–Palestine conflict, the Gansu earthquake, etc., have had a significant impact on human lives and caused incalculable property damage and casualties. After disasters and wars, the issue of rescuing large numbers of people becomes a problem that cannot be ignored. Due to the limited time available for rescue, rescue teams must complete the rescue operation as quickly as possible; otherwise, the chances of survival for the rescued people will be greatly reduced. Effective rescue is therefore essential [5].

In modern rescue operations, search and rescue robots play an important role [6]. Since disasters are likely to occur again at the rescue site during rescue operations, rescuers entering the scene may also be threatened, so rescue operations must be fast and accurate.

At present, robots used for post-disaster search and rescue can be divided into the following categories based on their mobility. First, the most common type is the tracked robot, such as AZIMUT [7], which has the ability to move in 3D space and also performs well in search and rescue operations, but its movement is relatively slow and it is difficult to enter the work area quickly. The Paripreksya2.0 [8] robot integrates a mechanical arm with four degrees of freedom, and tracks and four auxiliary foot paddles for movement, which can be used to perform various tasks. The VTM [9] is a robot that achieves multi-terrain and multi-directional movement through tracks and wheels, and it can carry a relatively high load. There is also a type of quadruped tracked robot that can traverse rough terrain using its legs and tracks, and can also use its legs as mechanical arms to perform some simple tasks [10]. Drones are also widely used in search and rescue operations due to their high maneuverability. For example, the University of California has developed an aerial deformable aircraft that can change shape by reversing the rotor [11]. The quadrotor MAV can dock on smooth walls and adapt to different working conditions [12]. Osaka University has developed a parallel linkage tilting flyer that can deform and pass through narrow areas [13]. C. Korpela et al. designed a flying vehicle with a robotic arm that can assist in performing some functions [14]. Na Zhao et al. [15,16] designed a quadcopter capable of aerial grasping; Carnegie Mellon University designed a modular snake robot that can move in multiple environments and has excellent obstacle avoidance capabilities, but its application in search and rescue is not satisfactory due to its driving method [17]. Professor Ye and his team at Shenyang Aerospace University designed a throwable spherical robot [18]. It has good mobility and can adapt to most environments. There are also some robots with multiple motion modes, such as HYTAQ [19] and FCSTAR [20], which have good maneuverability and can adapt well to unstructured environments. However, their structures are complex, costly and difficult to use on a large scale.

Although some of the robots mentioned above have strong maneuverability or certain advantages, they also have significant disadvantages. Some are too large in overall configuration, some cannot cross large obstacles, and some have difficulty entering work areas or have poor adaptability. Therefore, a new type of land–air omnidirectional mobile robot is proposed to open a new way for rescue and exploration missions. This robot can enter the work area through the flight system and transform to ground mode through mode switching. It can achieve omnidirectional movement on the ground without requiring additional power, even in confined areas. With its three modes of movement, it can change its shape at the appropriate time, reduce energy consumption, significantly increase working time, expand the working area, and adapt to unstructured environments.

## 2. Structure Design

### 2.1. Overall Configuration Design

This paper focuses on the design of a highly mobile, adaptable, and long-lived robot. The main idea is to combine different motion modes to propose a new type of land–air omnidirectional (LAOR) mobile robot that can change its structure to adapt to different environments while keeping the structure simple.

The LAOR robot mainly consists of a rotor–omnidirectional wheel composite structure. The outside of the rotor is surrounded by a single row of omnidirectional wheels, which are coupled to two sets of arms on a central base plate. The mode conversion structure allows the robot to switch between three modes, with the overall center of gravity just below the geometric center. Figure 1 shows the motion states of the robot in different scenarios, including omnidirectional movement on land, wall climbing, and airborne flight.

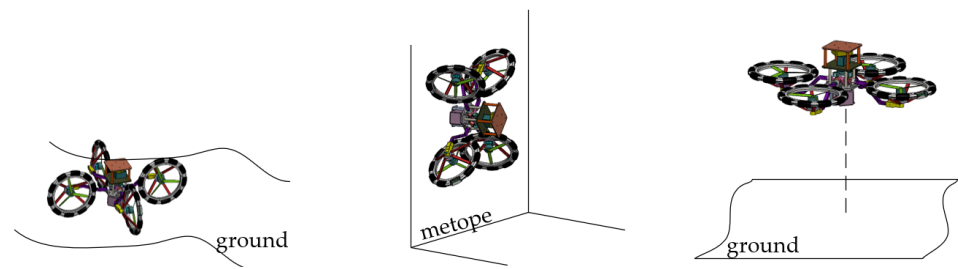


**Figure 1.** The motion states of an omnidirectional land–air mobile robot in different scenarios.

**2.2. Structure Design for Ground Movement Mode**

The first mode of operation of the all-terrain mobile robot is the ground movement mode. As shown in Figure 2, it is a three-dimensional structure diagram in the land motion mode, and the outline size is a 370.5mm square.

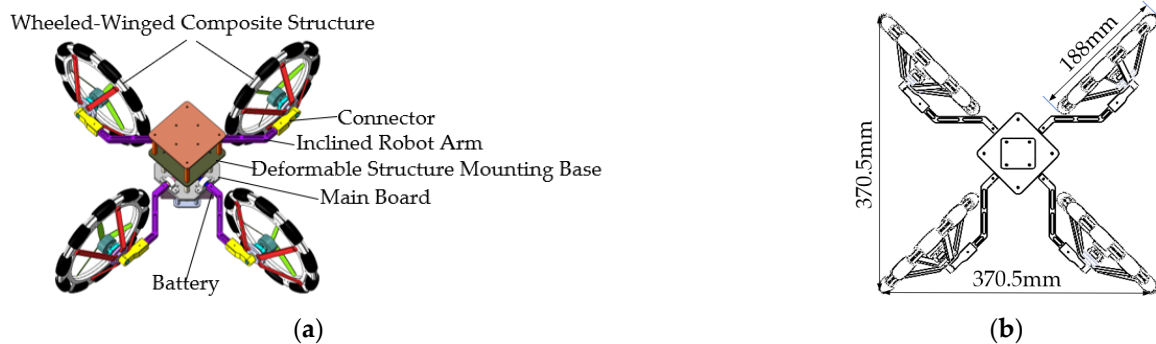


**Figure 2.** (a) Three-dimensional structural diagram; (b) basic dimensional drawing.

The schematic diagram of the omnidirectional wheel is as shown in Figure 3. The entire omnidirectional wheel consists of 10 small rollers, with a shaft sleeve embedded on each side of the roller to make the roller rotate more smoothly and reduce the overall vibration. The roller shafts are fixed to the omnidirectional wheel frame by limits, forming the outer contour of the omnidirectional wheel. Since the omnidirectional wheel needs to rotate as a whole, the seat of the brushless motor needs to be installed on the ground to achieve movement in all directions while walking and to be easy to control, so the rotor and inner ring of the omnidirectional wheel need to be in the same plane. For this reason, an arm-sinking structure is adopted, and the outer contour of the omnidirectional wheel is connected to the bearing seat by oblique spokes. Thin-walled bearings are limited by snap rings in the bearing seat for rotation of the omnidirectional wheel. In this way, four individual omnidirectional wheels plus the center frame form the overall structure for ground movement.

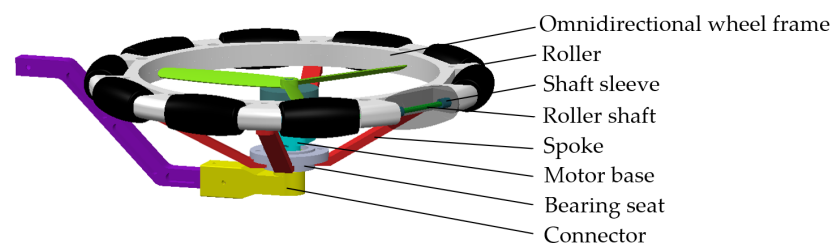


**Figure 3.** Three-dimensional model of a single wheeled–winged composite structure.

**2.3. The Structure Design for the Wall Climbing Mode**

In order to keep the robot simple and light, the structure for the wall climbing mode is designed without any additional components. As the robot moves along the wall, it needs

a force to hold on to the wall, which is perpendicular to the wall and is generated by the rotor. This force forms a  $75^\circ$  angle with the wall. As shown in Figure 4 LAOR's movement on the wall can be achieved in the following ways: up and down, left and right. (In the figure,  $F_{1-4}$  are equal effects produced by rotor rotation, as shown below.)



**Figure 4.** (a) Three-dimensional structural diagram; (b) basic dimensional drawing.

#### 2.4. Structure Design for Aerial Flight Mode

To achieve aerial flight functionality, the design adopts an 'X'-shaped quadcopter structure. This design is simple, easy to control, and has low manufacturing costs, making it an ideal choice for stable aerial flight. Firstly, the 'X' layout ensures high stability during flight, allowing the aircraft to maneuver easily in complex environments and achieve excellent agility. Secondly, the structure of this layout is relatively simple and easy to manufacture. Most importantly, the 'X'-shaped quadcopter design is highly reliable and flexible, enabling efficient task execution in various application scenarios. Figure 5 shows an exploded view of the flight system.

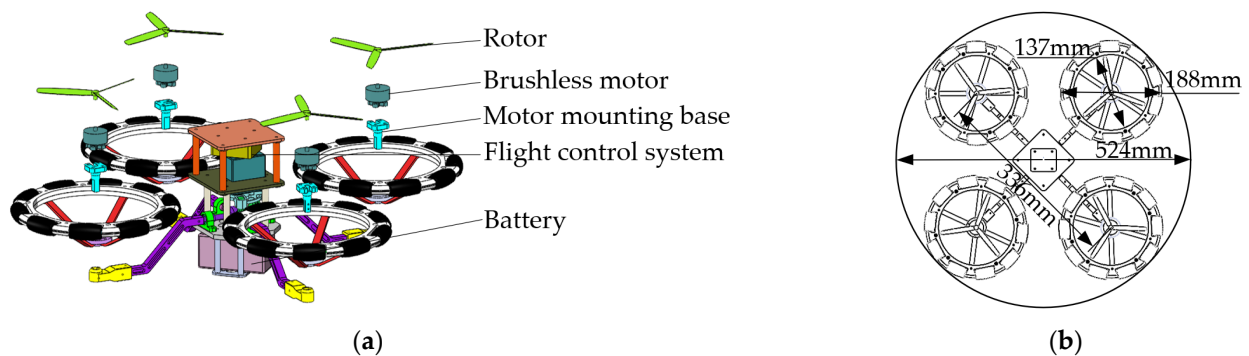


**Figure 5.** (a) Exploded view diagram of aerial flight mode; (b) basic dimensional drawing.

The robot's symmetrical structure places the overall center of mass directly below the horizontal center of the four rotors, which helps maintain balance, simplifies control, and allows for more stable and agile flight.

#### 2.5. Mode Switching Structure Design

The structure shown in Figure 6 is an X-shaped cross-rotating deformation structure, which mainly consists of servo motors, servo motor mounting plates, columns, turntables, movable blocks, movable vertical shafts, bearings, bearing seats, and two cross-rotating central rotating shafts, one inside and one outside. This structure is an actively deformable structure, with the turntable driven to rotate by servo motors. The grooves on the turntable can limit the movable shaft, so when the turntable rotates, the movable shaft inside the groove can rotate the inner and outer two central shafts simultaneously ( $0\sim 90^\circ$ ). The movable shaft and the movable block are connected to the two central shafts, respectively,



allowing the two central shafts to rotate, thereby switching between the antenna mode and the ground mode.

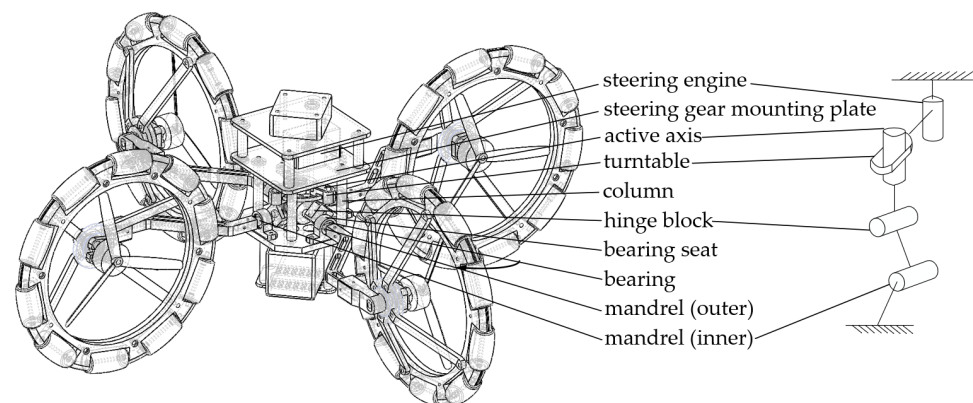


**Figure 6.** Schematic diagram of a model transformation structure.

### 2.6. Advantage Analysis

The durability of drones is crucial, especially when combining different functionalities. The key is to keep the structure simple to overcome the challenge of increased weight in hybrid drones. This paper presents a novel multi-mode mobile robot whose most prominent feature is the wing–wheel hybrid structure. This structure allows the robot to move omnidirectionally on the ground, perform typical quadcopter functions in the air, and perform a range of climbing actions on walls.

In order to extend the lifetime of the robot, the design needs to be simplified while still ensuring that the robot can perform its basic functions. Therefore, we propose the wing–wheel hybrid structure. The basic characteristic of this structure is that the rotors are covered by omnidirectional wheels, and both the rotors and the wheels are coaxial. The omnidirectional wheels can act as wheels for surface movement and as protective covers for the rotors, effectively shielding them during collisions.

The novelty of this design is that the omnidirectional land–air mobile robot can generate thrust in different directions with its four rotors while moving on the ground and walls. By combining thrusts in four different directions, it can generate propulsive forces in any direction, allowing omnidirectional movement on the ground with continuously changing wheels. This design achieves three modes of motion without adding weight, reducing space requirements and simplifying the overall structure, making it lighter and more comfortable. In addition, the offset structure of the rotation axes of the omnidirectional wheels and the contact points with the ground makes the robot easier to control in both ground and wall climbing modes.

When performing tasks, the robot may encounter different situations that require different modes of motion. However, the energy consumption varies between the different modes. The ground mode does not need to overcome gravity and therefore consumes the least energy, while the wall climbing and flight modes consume relatively more energy. It is therefore important to combine the movement modes wisely during use. The ground movement mode should be used when climbing or flying is not necessary to minimize unnecessary use and reduce energy consumption. When encountering obstacles or terrain unsuitable for ground movement, the robot can switch to wall climbing or flight mode, demonstrating its high adaptability.

### 3. Motion Analysis

The LAOR has three modes of movement, each of which requires precise control of its mechanisms.

In ground movement mode, since the four rotors must have diagonally opposite rotors rotating in the same direction while the adjacent rotors rotate in opposite directions to bal-

ance the torque generated by the rotors during flight, if motors 1 and 3 rotate clockwise and motors 2 and 4 rotate counterclockwise, the force generated by the rotors is as shown in the figure, with all four rotors generating equal forces, and the resulting force direction is along the positive Y-axis, as shown in Figure 7a, which represents the LAOR moving forward. Conversely, if all four rotors rotate in the opposite direction, they will produce equal forces in the opposite direction, as shown in Figure 7b, causing the LAOR to move backwards.

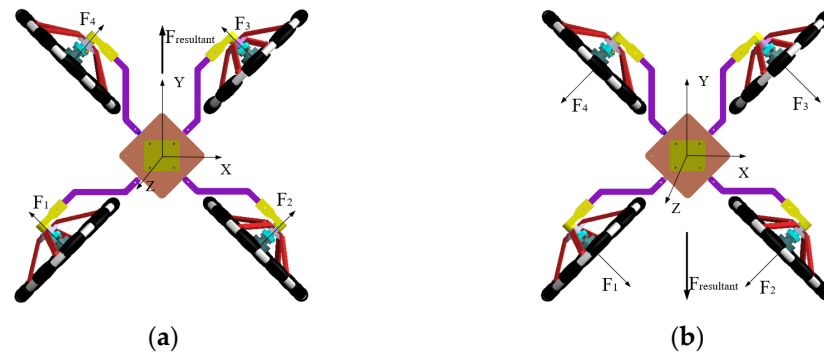


Figure 7. (a) LAOR forward movement; (b) LAOR backward movement.

To achieve the left and right movement mode of the LAOR, a set of diagonally opposite motors must change direction, thereby changing the direction of the resulting force. Building on the basis of forward movement, by reversing the direction of motors 1 and 3, the LAOR can move to the right, as shown in Figure 8a. Conversely, building on the basis of backward movement, by reversing the direction of motors 2 and 4, the LAOR can move to the left, as shown in Figure 9b.

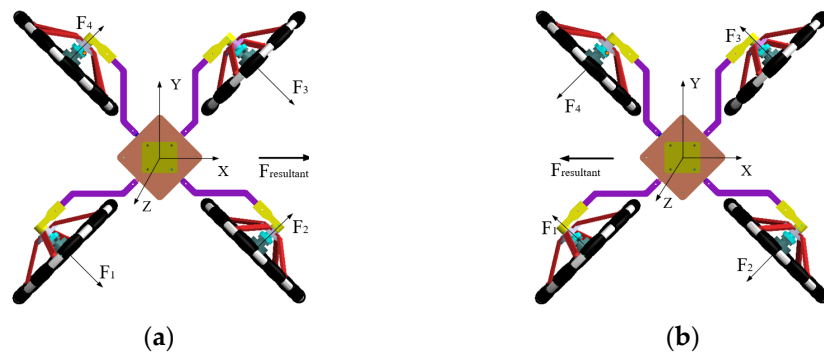


Figure 8. (a) LAOR rightward movement; (b) LAOR leftward movement.

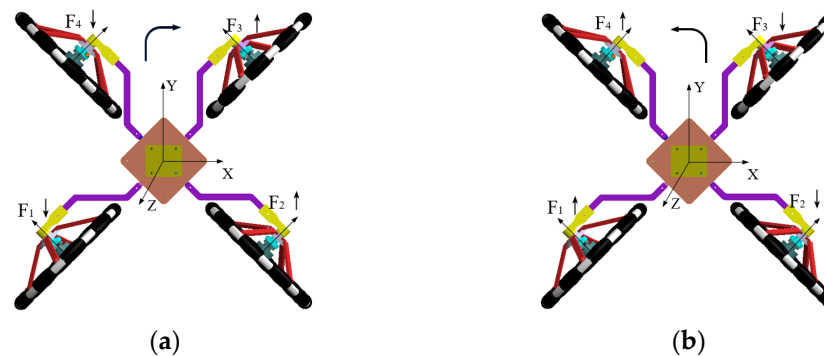


Figure 9. (a) LAOR right turn; (b) LAOR left turn.

To make the LAOR turn, the rotors are controlled in a similar way to a quadcopter. By increasing the speed of motors 2 and 3 while decreasing the speed of motors 1 and 4, the

rotors generate a force that causes the LAOR to turn to the right, as shown in Figure 10a. Conversely, by increasing the speed of motors 1 and 4 while decreasing the speed of motors 2 and 3, the rotors generate a force that causes the LAOR to turn to the left, as shown in Figure 9b.

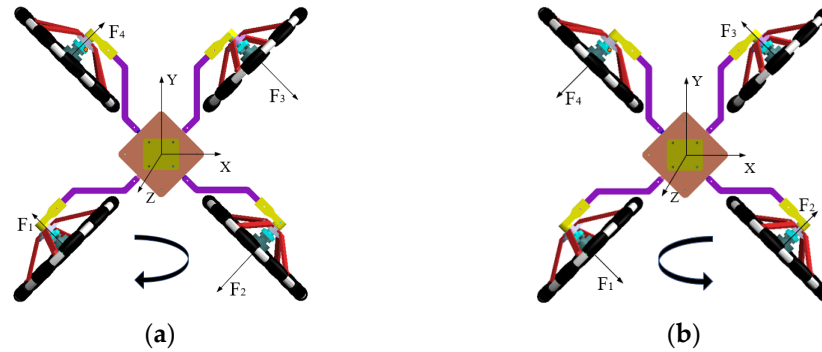


Figure 10. (a) LAOR clockwise pivot turn; (b) LAOR counterclockwise pivot turn.

To achieve LAOR’s spinning motion in place, the control method for the rotors is as shown in the figure. Building on the forward movement of LAOR, changing the direction of motors 2 and 3 so that all four rotors generate equal forces will cause LAOR to rotate clockwise in place, as shown in Figure 10a. Conversely, building on the backward movement of LAOR, changing the direction of motors 2 and 3 so that all four rotors generate equal forces will cause LAOR to rotate counterclockwise in place, as shown in Figure 10b.

Next is the wall climbing mode, where the robot requires an adhesive force to move on the wall, generated by the force of the rotor perpendicular to the wall, which requires a certain angle between the rotor–wheel composite structure and the wall. Figure 11 shows the force analysis of a single rotor–wheel composite structure.  $F_{deg}$  represents the resultant force generated by a single rotor,  $F_c$  is the force parallel to the wall,  $F_{ad}$  is the adhesive force that keeps the LAOR attached to the wall,  $F_{lift}$  is the lifting force perpendicular to the wall, and  $F_j$  is the vertical force required for vertical movement on the wall.

$$F_c = F_{deg} \cos\alpha \tag{1}$$

$$F_{ad} = F_{deg} \cos\beta \tag{2}$$

$$F_j = 4F_c \cos 15^\circ \cos 45^\circ \approx 2.73F_c \tag{3}$$

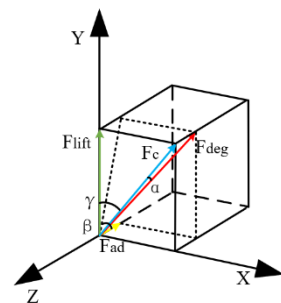


Figure 11. Analysis of the force on a single-rotor omnidirectional wheel.

If the robot is initially at rest on the wall,

$$F_j = G \tag{4}$$

When the speed of all four motors increases by the same amount,

$$F_{c1} = F_{c2} = F_{c3} = F_{c4} \tag{5}$$

$$F_j > G \tag{6}$$

At this point, LAOR moves vertically upwards, as shown in Figure 12a. When the speed of four motors decreases by the same amount,

$$F_{c1} = F_{c2} = F_{c3} = F_{c4} \tag{7}$$

$$F_j < G \tag{8}$$

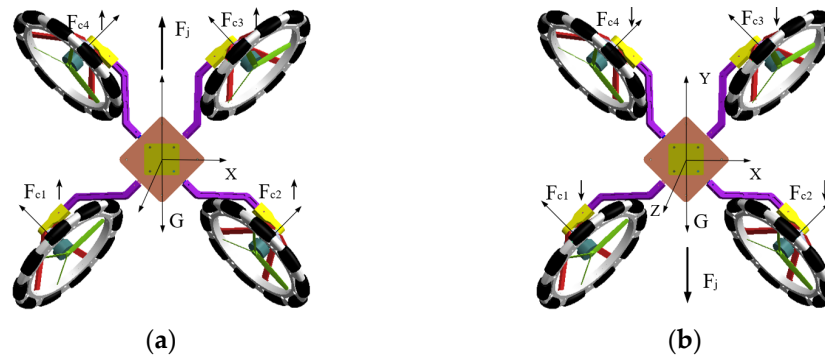


Figure 12. (a) LAOR ascending movement; (b) LAOR descending movement.

At this point, LAOR moves vertically downward, as shown in Figure 12b.

Movement along the wall also involves horizontal translation, with the initial state being equilibrium on the wall. At this point,  $F_j = G$ . To achieve lateral movement on the wall, LAOR needs to maintain  $F_j = G$ . To maintain a constant vertical height, as shown in Figure 13a, the control strategy for the four motors is as follows. Increase the speed of motors 2 and 4, and decrease the speed of motors 1 and 3, with the increase in speed of motors 2 and 4 equal to the decrease in speed of motors 1 and 3. Increase the speed of motors 1 and 3 and decrease the speed of motors 2 and 4, with the increase in speed of motors 1 and 3 being equal to the decrease in speed of motors 2 and 4. This will create a horizontal force to the left, allowing horizontal movement to the left, as shown in Figure 13b.

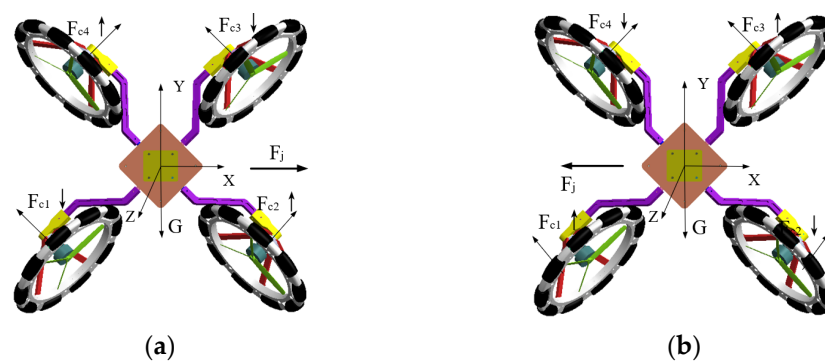


Figure 13. (a) LAOR rightward lateral movement; (b) LAOR leftward lateral movement.

The final mode is the LAOR’s airborne mode, where the quadrotor adopts an “X” configuration. The flight attitude of the quadrotor is in an “X” configuration, where the control involves adjusting the speed of all four motors simultaneously to control the flight attitude of the quadrotor.

#### 4. Prototype and Experiment

The overall control system structure is shown in Figure 14, using the SpeedyBee F7V3 as the main controller running the mainstream Betaflight flight control system. The system

executes the aircraft's movements, such as walking on the ground and climbing walls, through command line channel mixer control settings. The four-in-one BL32 brushless motor electronic speed controller can control the speed and direction of brushless motors and supports instantaneous direction changes, enabling omnidirectional operation on the ground and on walls. The digital servo has a single-pulse angle maintenance feature, which can maintain the set angle from the last control pulse given by the flight control system, thus avoiding dangerous situations caused by unstable aircraft shapes. The battery is a 22.2 V polymer lithium battery with a high discharge rate to increase the payload capacity of the aircraft.

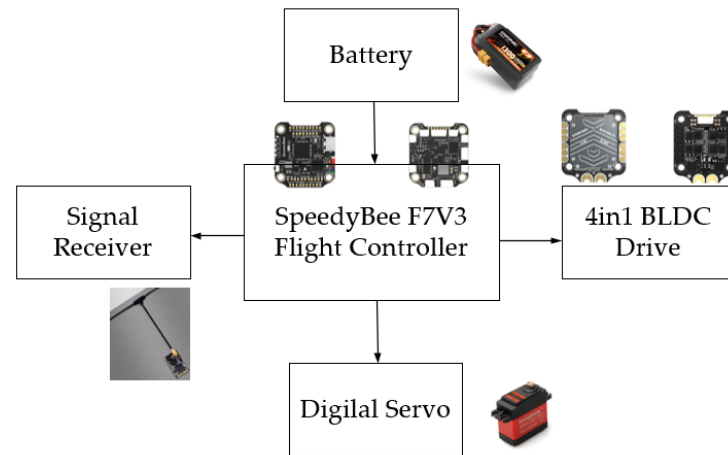


**Figure 14.** Overall control system architecture diagram.

Figure 15 shows an image of the LAOR prototype. The four wheels are a combination of propeller and wheels, with the omnidirectional wheel frame 3D-printed in ABS. The overall design is lightweight, yet the material provides sufficient strength. The omnidirectional wheels are made of rubber, which offers good wear resistance, elasticity, and grip. Key stressed parts are made from 7075 aluminum alloy.

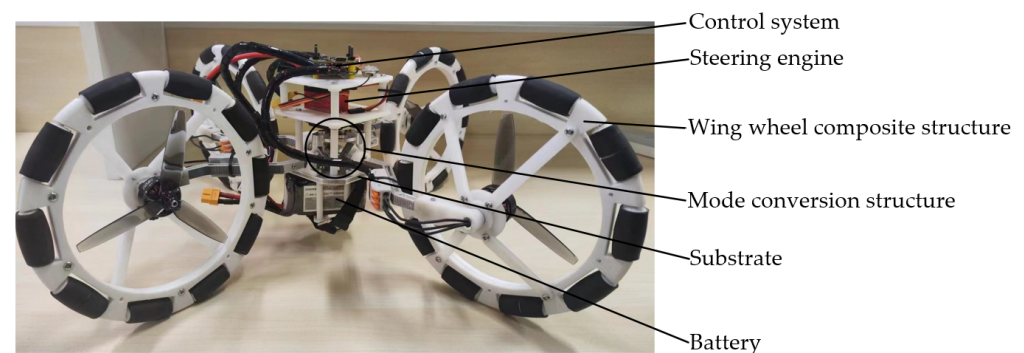


**Figure 15.** Deformed LAOR prototype in ground mode.

As shown in Table 1, the quality table of the LAOR prototype is the single-rotor omnidirectional wheel composite structure with the highest proportion, and the key components are made of aluminum alloy material to ensure the overall strength. Other components include the arm, flight control, etc., with a total mass of 1092.19 g.



**Table 1.** Prototype quality table.

Structure Name	Mass/g
Rotor–Omnidirectional wheel × 4	639.44
Flight controller + Electronic speed controller	29.9
Slanted arm × 4	57
Board × 4	118.85
Battery	213
Mode conversion structure	34

As shown in Figure 16, the land–air omnidirectional mobile robot has three modes of operation:

- When the wheels are perpendicular to the contact surface, it is in the ground motion mode.
- By passing through the mode conversion structure, the angle between the omnidirectional wheel and the contact surface can be adjusted. When the angle between the wheel and the contact surface is  $75^\circ$ , it is in the wall mode. The force generated by the rotating rotor has a component perpendicular to the wall, which allows the robot to stick to the wall. There is also a vertical force that causes the robot to move along the wall.
- When the wheels are parallel to the horizontal plane, it is in the aerial flight mode with an ‘X’ rotor distribution, providing flexibility in control and high motor efficiency.

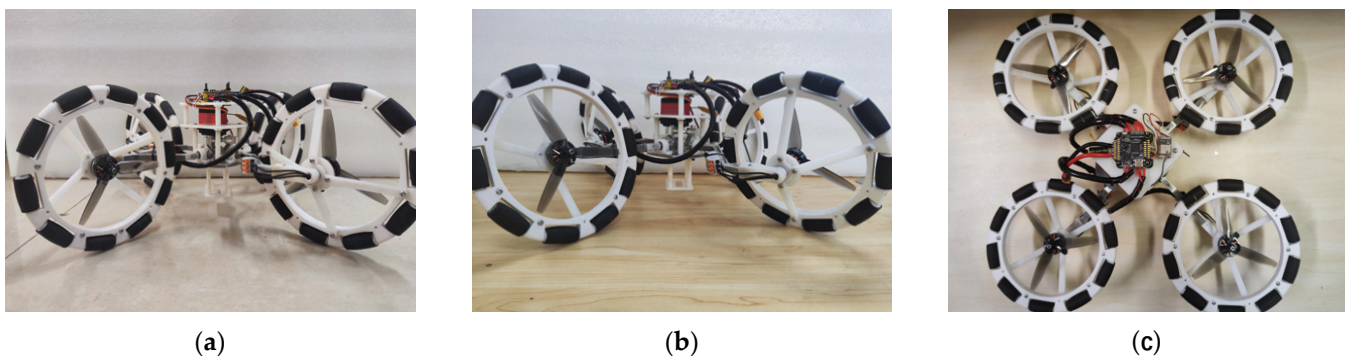


**Figure 16.** Assembly diagram of the prototype in three different modes; the above are (a) land mode, (b) wall mode, (c) air mode.

Based on the theory and the designed prototype, experiments were carried out. The experiments were divided into three main parts: ground motion, wall climbing, and aerial flight.

The novel multi-mode mobile robot is designed with impressive performance indicators, ensuring its versatility and efficiency across various tasks. It boasts a maximum aerial flight speed of 10 m/s and a maximum ground movement speed of 6 m/s. The robot can climb vertical surfaces at speeds up to 2 m/s and can reach a maximum flight altitude of 60 m and a climbing height of approximately 20 m. It supports a load capacity of up to 200 g, as shown in Table 2.

As shown in Table 3, LAOR is compared with drones and ground vehicles of similar sizes, including endurance and adaptability. Compared to drones and ground vehicles of similar sizes, LAOR falls between them in terms of endurance. While LAOR may not have the same endurance as similarly sized ground vehicles, its adaptability far exceeds that of traditional ground vehicles. LAOR’s multi-mode design allows it to operate flexibly in various environments such as ground, walls, and air, effectively meeting complex task requirements and environmental challenges.

**Table 2.** Performance capability table.

Performance Indicators	Values
Ground Movement Speed	up to 10 m/s
Wall Climbing Speed	up to 6 m/s
Aerial Flight Speed	up to 2 m/s
Load Capacity	up to 200 g
Maximum Flight Altitude	60 m
Maximum Climbing Altitude	20 m
Wind Resistance	4 Beaufort scale

**Table 3.** Performance comparison table.

	LAOR	Same Size Drone	Same Size Rover
Endurance	20–23 min	10–12 min	30 min
Adaptability	high	medium	low

The ground movement experiment was crucial to ensure that the land–air omnidirectional mobile robot could achieve omnidirectional movement on the ground. The experiment was conducted indoors on a flat surface, following a square path to ensure that the robot could move in all directions on the ground. The experiment recorded the robot’s trajectory over time and generated a trajectory map for the land–air omnidirectional mobile robot.

As shown in Figure 17, the land–air omnidirectional mobile robot follows a square trajectory, moving clockwise to complete forward movement, right lateral movement, backward movement, and left lateral movement. To achieve omnidirectional motion on the ground, the robot must also perform a rotation in place. As shown in Figure 18, the flexibility test of LAOR’s ground movement is performed in a figure-eight trajectory, demonstrating its high flexibility.

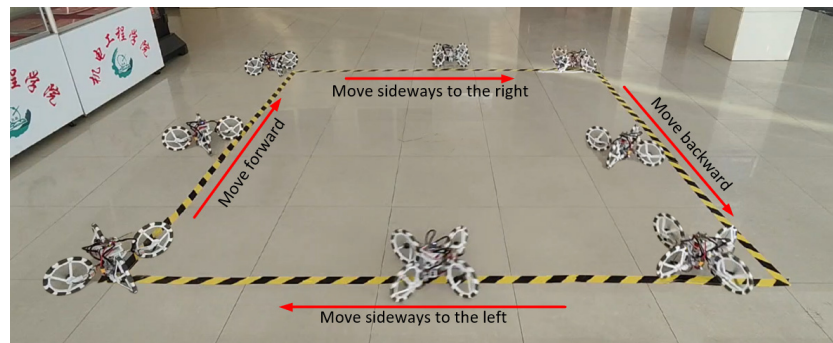


**Figure 17.** LAOR omnidirectional movement of land experiment.

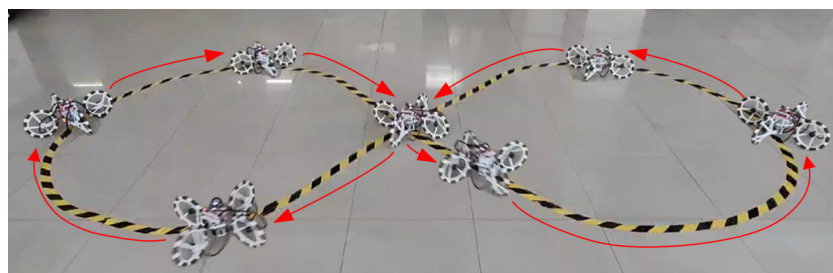


**Figure 18.** LAOR ground ∞ track test.

To obtain the land motion-related data of the omnidirectional mobile robot, an outdoor land motion test was conducted next. The open ground was selected for the test. Figure 19

shows the trajectory diagram of the outdoor land motion test robot. Taking the initial position in the figure as the starting point, the robot moves forward and reaches the middle position. Currently, a set of diagonal rotors of the robot are controlled to reverse and start to move horizontally to the left. The data collection experiment is completed when it moves to the end position.

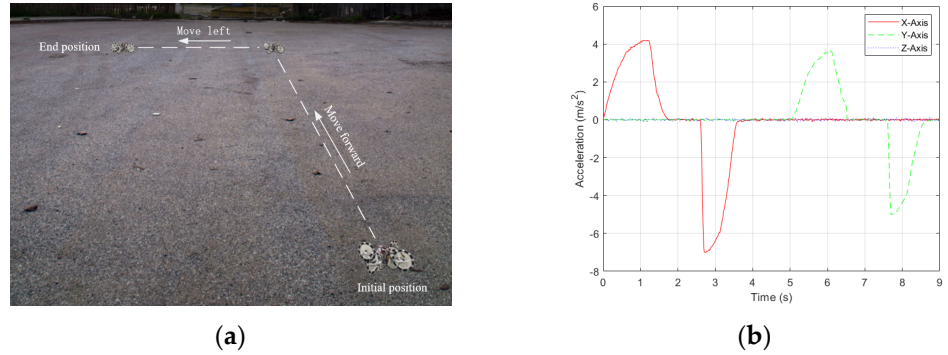


**Figure 19.** (a) LAOR outdoor mobile experiment; (b) time-acceleration relationship curve for outdoor land sports.

After processing the data measured by the three-axis accelerometer, the land motion time–acceleration curve is obtained, as shown in Figure 19. The X-axis acceleration data are the acceleration data in the forward direction. The acceleration in the X-axis direction increases first and then decreases in the acceleration stage. At 1.8 s, the robot enters a uniform motion state, which lasts for about 0.7 s. When entering the deceleration state, the reverse acceleration suddenly increases, because the deceleration uses a reverse motor steering, which can respond to deceleration more quickly. At about 5 s, the robot begins to move horizontally, which is the change in the Y-axis acceleration. The results show that the robot runs smoothly, meets the expected effect, and has good motion performance on land.

The aim of the wall climbing experiment is to get the robot to move up, down, and sideways on a wall. An indoor wall was chosen for the experiment. Figure 20a shows the trajectory of the land–air omnidirectional mobile robot on the wall. Points 1 and 2 represent the up and down movements of the robot on the wall, while points 3 and 4 represent the lateral movements of the robot on the wall. The collected acceleration data are organized into a curve chart, as shown in Figure 20b. It can be calculated that in the wall movement experiment, the robot moves upward at a uniform speed of about 2.5 m/s. At the same time, it is not difficult to see that the robot will be bumpy during the movement and may deviate from the pre-set path.

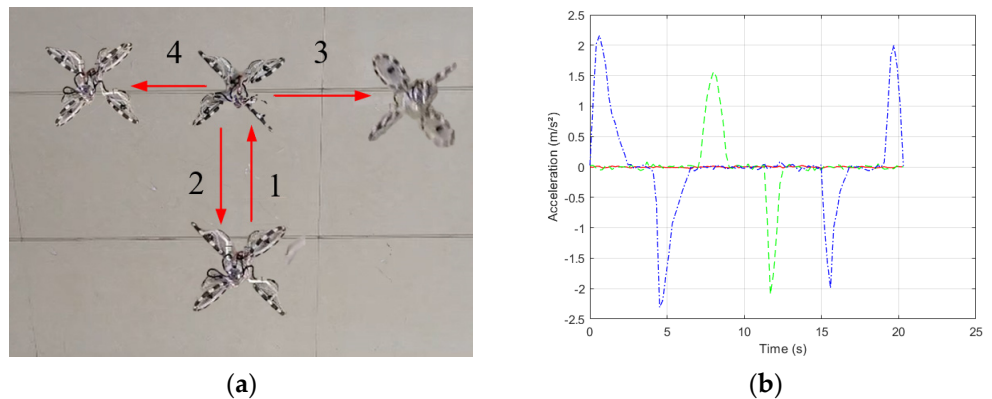


**Figure 20.** (a) LAOR wall crawling experiment; (b) time-acceleration relationship curve for outdoor land sports.

The wall crawling test provides an important reference for the practical application of the robot on the wall. In the design of the next generation of robots, the structure and control algorithm of the robot will continue to be improved to improve its performance in the wall crawling mode and ensure its stable operation in complex environments.

The aerial flight experiment involves the land–air omnidirectional mobile robot performing vertical take-off and landing, hovering in place, rotating in place and turning, and flying forward, backward, left, and right. Figure 21 shows the flight trajectory for the airborne experiment, ensuring that all airborne functions can be achieved.

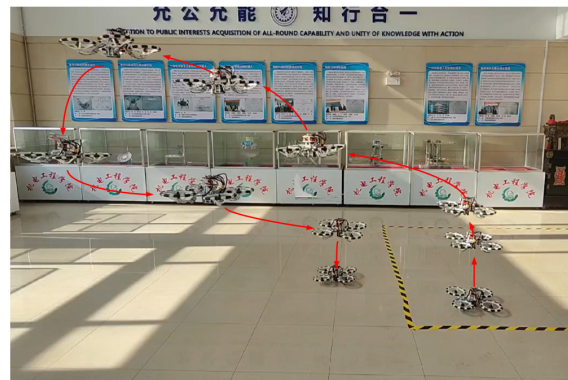


Figure 21. LAOR aerial flight experiment.

To obtain the outdoor flight experimental data of the drone, an outdoor flight test is required. As shown in Figure 22a, the outdoor test is carried out in a safe environment with a wind speed of 3 to 4.

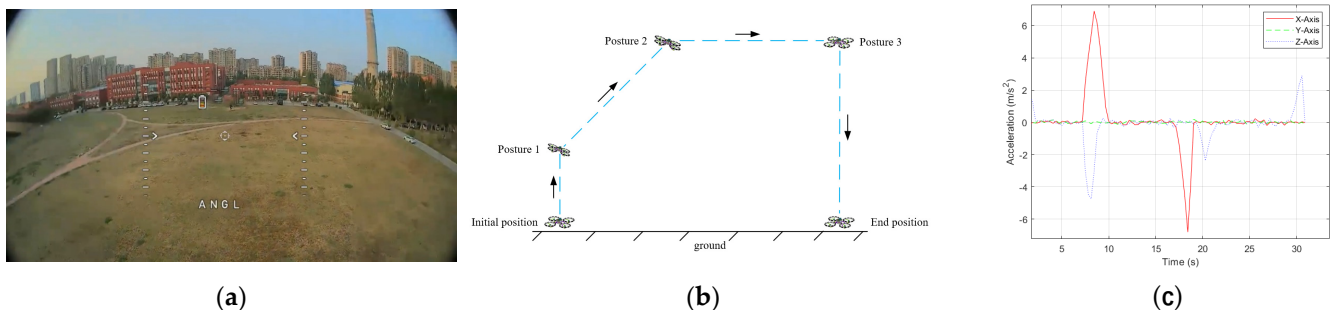


Figure 22. Outdoor flight experiment; the above are (a) track map, (b) aerial view, (c) time-acceleration relationship curve.

As shown in Figure 22b, the outdoor flight test trajectory of the land–air omnidirectional mobile robot is schematically shown. From the initial position point to posture 1, the robot is in a vertical take-off state. Posture 1 is the robot flying obliquely upward. From posture 2 to posture 3, the robot is flying forward horizontally. When it reaches posture 3, it starts to land vertically.

As shown in Figure 22c, the relationship between time and acceleration of the outdoor flight test of the land–air omnidirectional mobile robot corresponds to each stage in Figure 22b. Among them, 0~7 s is the process of vertical take-off. The acceleration of the Z axis increases first and then decreases. Currently, the robot accelerates vertically upward. Between 7 and 10 s, it corresponds to the transformation from posture 1 to posture 2. Between 10 and 16 s, the robot flies horizontally forward at a uniform speed. From 16 to 18.5 s, the robot decelerates and flies. From 18.5 s, the robot enters the landing state. The robot accelerates rapidly in the horizontal flight state, and the speed rises rapidly to about 10 m/s in a short time. The speed remained relatively stable at the peak, indicating that the UAV has good stability in high-speed flight. During the test, the acceleration curve showed

slight fluctuations, which may be due to environmental factors, adjustments to the flight control system, and airflow. Overall, the test results verified the superior performance of the UAV design in terms of speed and stability, providing strong support for further optimization and practical application.

## 5. Conclusions

This paper presents a deformable land–air omnidirectional mobile robot that includes omnidirectional movement on land, wall climbing, and aerial flight. It achieves mode conversion between air, land, and wall modes by a central cross-rotating structure. Each rotor is surrounded on the outside by a single row of continuous switching wheels. No additional power is required for ground and wall travel. Through structural design, motion analysis, and experimental verification, the robot's omnidirectional ground movement, excellent wall climbing ability, and aerial flight capability are fully demonstrated. Relevant experiments have been conducted in various environments, demonstrating the robot's high maneuverability and strong environmental adaptability. This enables the robot to perform a wide range of operations in unknown and unstructured environments, expanding its application in exploration and rescue fields. It can greatly improve the efficiency and portability of search and rescue robots.

## 6. Future Work

Based on the foundation of this study, there are many directions for further exploration and optimization. Future work will focus on the following aspects:

- (1) Further optimization of multi-mode switching technology: Although we have achieved switching between ground, wall, and aerial modes, there is still room for improvement. We plan to enhance switching speed and stability through more precise control strategies and sensor integration.
- (2) Enhancement of perception and navigation capabilities: Future research will aim to enhance the robot's perception capabilities, including environmental awareness and obstacle detection. We will explore advanced vision and navigation systems to improve the robot's navigation accuracy and safety in complex environments.
- (3) Expansion of application scenarios: The next steps will involve validation and expansion of the robot's applications in real-world scenarios. We will focus on exploring the robot's potential applications in rescue missions, environmental monitoring, and structural inspections to validate its effectiveness and applicability in practical tasks.

Through these explorations and optimizations in future work, we aim to further advance the development of multi-mode mobile robot technology, opening new possibilities and opportunities for future intelligent robot applications.

## 7. Patents

The invention relates to a rotor-driven deformable space–ground omnidirectional motion robot and a motion method (preliminary trial stage).

**Author Contributions:** Conceptualization, C.Y.; methodology, C.Y. and H.W.; prototype, H.W.; writing—original draft preparation, R.Z.; writing—review and editing, S.Y. and X.M.; supervision, X.M. and S.Y.; project administration, X.M. All authors have read and agreed to the published version of the manuscript.

**Funding:** This research was funded by the Research on Liaoning Provincial Natural Science Foundation (Grant no.20180520033).

**Data Availability Statement:** The original data contributions presented in the study are included in the article; further inquiries can be directed to the corresponding authors.

**Conflicts of Interest:** The authors declare no conflicts of interest.



## References

1. Mertyüz, İ.; Tanyıldızı, A.K.; Taşar, B.; Tatar, A.B.; Yakut, O. FUHAR: A transformable wheel-legged hybrid mobile robot. *Robot. Auton. Syst.* **2020**, *133*, 103627. [\[CrossRef\]](#)
2. Salamina, L.; Gaidano, M.; Melchiorre, M.; Mauro, S. Mobile Robot with Robotic Arm: Development and Validation of a Digital Twin. In Proceedings of the ASME 2023 International Mechanical Engineering Congress and Exposition, New Orleans, LA, USA, 29 October–2 November 2023; Advanced Manufacturing; Volume 3, p. V003T03A064.
3. Taheri, H.; Mozayani, N. A study on quadruped mobile robots. *Mech. Mach. Theory* **2023**, *190*, 105448. [\[CrossRef\]](#)
4. Kamegawa, T.; Akiyama, T.; Sakai, S.; Fujii, K.; Une, K.; Ou, E.; Matsumura, Y.; Kishutani, T.; Nose, E.; Yoshizaki, Y.; et al. Development of a separable search-and-rescue robot composed of a mobile robot and a snake robot. *Adv. Robot.* **2020**, *34*, 132–139. [\[CrossRef\]](#)
5. Murphy, R.R. Marsupial and shape-shifting robots for urban search and rescue. *IEEE Intell. Syst. Their Appl.* **2000**, *15*, 14–19. [\[CrossRef\]](#)
6. Bharathi, B.; Suchitha, B. Design and Construction of Rescue Robot and Pipeline Inspection Using Zigbee. *Int. J. Sci. Eng. Res.* **2013**, *1*, 75–78.
7. Michaud, F.; Letourneau, D.; Arsenault, M.; Bergeron, Y.; Cadrin, R.; Gagnon, F.; Legault, M.A.; Millette, M.; Pare, J.F.; Tremblay, M.C.; et al. AZIMUT, a leg-track-wheel robot. In Proceedings of the 2003 IEEE/RSJ International Conference on Intelligent Robots and Systems (IROS 2003) (Cat. No.03CH37453), Las Vegas, NV, USA, 27–31 October 2003; Volume 3, pp. 2553–2558.
8. Megalingam, R.K.; Vadivel, S.R.R.; Rajendraprasad, A.; Raj, A.; Baskar, S.; Balasubramani Marutha Babu, R. Development and evaluation of a search-and-rescue robot Paripreksya 2.0 for WRS 2020. *Adv. Robot.* **2022**, *36*, 1120–1133. [\[CrossRef\]](#)
9. Ben-Tzvi, P.; Saab, W. A Hybrid Tracked-Wheeled Multi-Directional Mobile Robot. *J. Mech. Robot.* **2019**, *11*, 041008. [\[CrossRef\]](#)
10. Biswal, P.; Mohanty, P.K. Development of quadruped walking robots: A review. *Ain Shams Eng. J.* **2021**, *12*, 2017–2031. [\[CrossRef\]](#)
11. Bucki, N.; Tang, J.; Mueller, M.W. Design and Control of a Midair-Reconfigurable Quadcopter Using Unactuated Hinges. *IEEE Trans. Robot.* **2023**, *39*, 539–557. [\[CrossRef\]](#)
12. Kalantari, A.; Mahajan, K.; Ruffatto, D.; Spenko, M. Autonomous perching and take-off on vertical walls for a quadrotor micro air vehicle. In Proceedings of the 2015 IEEE International Conference on Robotics and Automation (ICRA), Seattle, WA, USA, 26–30 May 2015; pp. 4669–4674.
13. Sakaguchi, A.; Takimoto, T.; Ushio, T. A Novel Quadcopter with A Tilting Frame using Parallel Link Mechanism. In Proceedings of the 2019 International Conference on Unmanned Aircraft Systems (ICUAS), Atlanta, GA, USA, 11–14 June 2019; pp. 674–683.
14. Korpela, C.; Orsag, M.; Oh, P. Towards valve turning using a dual-arm aerial manipulator. In Proceedings of the 2014 IEEE/RSJ International Conference on Intelligent Robots and Systems, Chicago, IL, USA, 14–18 September 2014; pp. 3411–3416.
15. Zhao, N.; Luo, Y.; Deng, H.; Shen, Y. The deformable quad-rotor: Design, kinematics and dynamics characterization, and flight performance validation. In Proceedings of the 2017 IEEE/RSJ International Conference on Intelligent Robots and Systems (IROS), Vancouver, BC, Canada, 24–28 September 2017; pp. 2391–2396.
16. Zhao, N.; Luo, Y.; Deng, H.; Shen, Y.; Xu, H. The Deformable Quad-Rotor Enabled and Wasp-Pedal-Carrying Inspired Aerial Gripper. In Proceedings of the 2018 IEEE/RSJ International Conference on Intelligent Robots and Systems (IROS), Madrid, Spain, 1–5 October 2018; pp. 1–9.
17. Lipkin, K.; Brown, I.; Peck, A.; Choset, H.; Rembisz, J.; Gianfortoni, P.; Naaktgeboren, A. Differentiable and piecewise differentiable gaits for snake robots. In Proceedings of the 2007 IEEE/RSJ International Conference on Intelligent Robots and Systems, San Diego, CA, USA, 29 October–2 November 2007; pp. 1864–1869.
18. Ye, C.; Ma, G.; Ma, S. Development of a throwable shape-shifting spherical robot. In Proceedings of the 2014 IEEE International Conference on Mechatronics and Automation, Tianjin, China, 3–6 August 2014; pp. 641–645.
19. Kalantari, A.; Spenko, M. Design and experimental validation of HyTAQ, a Hybrid Terrestrial and Aerial Quadrotor. In Proceedings of the 2013 IEEE International Conference on Robotics and Automation, Karlsruhe, Germany, 6–10 May 2013; pp. 4445–4450.
20. David, N.B.; Zarrouk, D. Design and Analysis of FCSTAR, a Hybrid Flying and Climbing Sprawl Tuned Robot. *IEEE Robot. Autom. Lett.* **2021**, *6*, 6188–6195. [\[CrossRef\]](#)

**Disclaimer/Publisher’s Note:** The statements, opinions and data contained in all publications are solely those of the individual author(s) and contributor(s) and not of MDPI and/or the editor(s). MDPI and/or the editor(s) disclaim responsibility for any injury to people or property resulting from any ideas, methods, instructions or products referred to in the content.